

Rapid Method of Mapping Eddy Current Fields

Andrew J Wheaton¹ and Wayne R Dannels¹

¹Toshiba Medical Research Institute USA, Mayfield, OH, United States

INTRODUCTION

Despite advances in gradient hardware, including shielded gradient coil designs and pre-emphasis [1], residual eddy current fields persist in modern commercial MR scanners. These residual fields can include zeroth (B_0), linear (X, Y, Z) and higher order spatial terms (Z^2 , XY, X^2-Y^2 , etc.). For most applications, residual eddy fields have a negligible effect on image quality. However, some sequence applications like Diffusion-weighted EPI (DW-EPI) are sensitive to these eddy fields [2-6]. Methods exist to compensate DW-EPI either in reconstruction [2] or by fine adjustment of gradient moments, frequency offsets, and receiver phase [3]. However, these compensation methods address only zeroth and/or linear eddy terms. Recent studies have emphasized the effects on DW-EPI of the remaining uncompensated higher order eddy terms on and demonstrated methods for their correction [4,5].

To correct linear and/or higher order eddy fields, a measurement or model of the spatial distribution of the eddy fields is necessary. Existing methods of volumetric field mapping [4-6] typically acquire only one phase encode per TR, which can be slow if TR is long. The purpose of this investigation is to develop a tool to rapidly generate a volumetric map of eddy current fields, including linear and higher order spatial terms.

EDDY CURRENT MAPPING METHOD

ACQUISITION

The eddy current mapping method utilizes a prepulse module consisting of pair of nonselective RF pulses separated by a gradient lobe (GR_{tag}); an arrangement most commonly used for grid tagging (Figure 1). Preceding the grid tag module is an eddy current-generating stimulus consisting of a simple gradient lobe. Any eddy current field generated by the stimulus will result in additional moment accumulation during the interpulse period (τ) of the grid tag module. This added moment will warp the spatial pattern of the grid lines; the spatial warping pattern being directly related to the spatial distribution of the eddy fields. The image data is read out using any conventional sequence; for efficiency, a rapid method like fast spin-echo may be used.

PROCESSING

The effect of the eddy-generated moment is to spatially warp the grid tag lines (Figure 2). An eddy component in the same direction as the grid tag gradient (self-terms, e.g. YeY) results in a dilation or compression of the grid tag lines. An eddy component in the orthogonal direction (cross-terms, e.g. YeX) generates a rotation of the grid tag lines. The dilation/compression and/or rotation occur locally depending on the local spatial distribution of the eddy terms.

The spatial warping could be measured in the image domain using image processing methods. However, for simplicity, the warping can be processed in k-space using methods similar to Ref. 7. The sinusoidal modulation of image space by the grid tag module produces spatial harmonics in k-space. If the grid spacing is X cm, three 'replicants' of k-space are produced, centered at 0 ('center'), $+X^{-1}$ ('right'), and $-X^{-1}$ ('left'), respectively. These three replicants can be separated using bandpass filters and reconstructed into individual complex images. The phase image (θ) of each replicant is calculated using a simple arctangent. The off-resonance phase map is calculated by the subtraction $\theta_{off} = (\theta_{right} - \theta_{left}) / 2$. The off-resonance phase due to eddy-related sources only can be calculated by subtracting the off-resonance phase map calculated from a reference data set ($\theta_{eddy} = \theta_{off} - \theta_{ref}$). The eddy field map for a given stimulus in a chosen direction (e.g. XeY is X-axis stimulus in the Y direction) is calculated as the spatial derivative of the eddy phase map generated by each stimulus (e.g. θ_{eddyX} and θ_{eddyY}) (Equation 1).

EXPERIMENTAL METHODS

The residual eddy current fields were measured on a wide-bore 3T clinical scanner. Conventional eddy current pre-emphasis (previously calibrated) was enabled; hence, the residual eddy currents were measured. A 30 cm sphere containing mineral oil was positioned at isocenter in the magnet bore. The eddy current mapping method was repeated to acquire three data sets: reference (stimulus off), X-axis stimulus, and Y-axis stimulus. Both gradient stimuli were 30 mT/m trapezoidal lobes with zero delay between the end of the falling ramp of the gradient and the grid tag module. The gradient stimulus duration was 1s to allow any eddy currents from the initial gradient rise to decay to make the experiment sensitive only to the falling ramp of the trapezoid. A two-shot asymmetric fast spin-echo readout was used with a TR of 3 s. Thus, a single slice was acquired in 6 s per data set, or 18 s for the whole experiment.

RESULTS

Representative eddy current maps are displayed in Figures 2 and 3. The maps demonstrate higher order spatial dependence that can be described by spherical harmonics: $XeX: A \cdot y^2$, $XeY: A \cdot xy$, $YeX: -A \cdot xy$, $YeY: A \cdot x^2$. At isocenter ($x=y=0$), the amplitude of all eddy fields falls to zero due to (previous) proper calibration of the linear terms for pre-emphasis correction.

DISCUSSION

Eddy currents generated by the readout sequence itself do not influence the measurement since the eddy field is calculated by processing the spatial harmonics of the grid pattern, not raw image data. Thus, the stimulus, sensitization, and detection elements of the eddy current measurement are effectively decoupled and hence can be optimized separately. The stimulus amplitude and physical axis can be chosen freely. Time-dependency can be introduced by adjusting the delay between the stimulus and the grid tag module and repeating the experiment. Sensitivity to eddy fields can be tuned by modifying the interpulse duration (τ) of the grid tag module. The τ period effectively acts like an integration of the eddy-generated moment during that interpulse duration. The longer the τ period, the more sensitive the experiment is to eddy-related sources. However, due to the effective integration of the eddy field during the interpulse period, the accuracy of measuring short-term eddy components (with time constants $\ll \tau$), which may decay during this time, is compromised. The readout sequence can be 2D or 3D of any type (field-echo, spin-echo, etc.) and can be optimized separately based on the conventional trade-offs of image resolution, signal-to-noise, and time-efficiency.

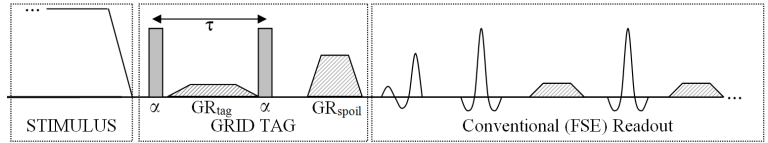


Figure 1. Pulse sequence diagram for eddy current mapping method. An initial eddy-generating stimulus is followed by a grid tag module for sensitization. The grid tag spatial modulation is detected using a conventional sequence, (e.g. fast spin-echo).

The grid tag spatial modulation is detected using a conventional sequence, (e.g. fast spin-echo).

$$\begin{aligned} XeX(x, y) &= \frac{\partial \theta_{eddyX}(x, y)}{\partial x} & YeX(x, y) &= \frac{\partial \theta_{eddyY}(x, y)}{\partial x} \\ XeY(x, y) &= \frac{\partial \theta_{eddyX}(x, y)}{\partial y} & YeY(x, y) &= \frac{\partial \theta_{eddyY}(x, y)}{\partial y} \end{aligned} \quad \text{Equation 1}$$

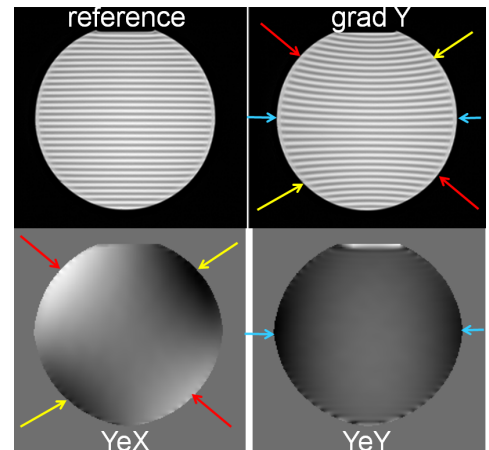


Figure 2. Illustration of the effect of eddy current fields on spatial grid tag lines for a Y-axis stimulus. A reference image is provided for comparison. Self-terms (YeY) generate dilation (blue arrows) Cross-terms (YeX) generate rotations, either clockwise (red arrows) or counter-clockwise (yellow arrows), depending on the polarity of the field. On the eddy map data, white = positive amplitude, black = negative, and gray = zero.

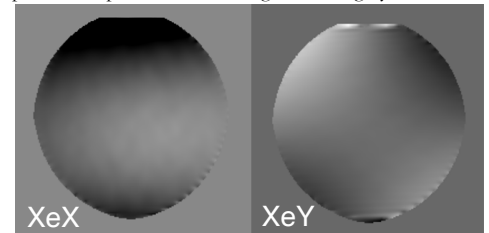


Figure 3. Eddy current field maps for XeX and XeY .

- REFERENCES** 1. Glover G, Pelc N. US Patent 4,698,591 (1987). 2. Haselgrove JC, Moore J. MRM 1996;36:960-964. 3. King K, Ganin A. US Patent 6,025,715 (2000). 4. Xu D, Maier J, King K, et al. ISMRM 2011; p4564. 5. Xu D, Maier J, King K. ISMRM 2012; p4163. 6. Boesch C, Gruetter R, Martin E. MRM 1991; 20:268-284. 7. Dannels W, Wheaton AJ. US Patent 8,077,955 (2011).